# Integration of Promoter and Exon Arrays for colorectal carcinoma cell line shows pathways of neurodegenerative diseases are over-represented under Oxaliplatin treatment

Yi-An Ko<sup>1\*</sup>, Feng-Hsiang Chung<sup>1\*</sup>, Hong-Da Chen<sup>1</sup>, Chih-Hao Chen<sup>1,2</sup>, Hsing-Chung Lee<sup>2</sup>, Akon Higuchi<sup>3,4</sup>, Qingdong Ling<sup>1,2\*</sup>, and HC Lee<sup>1,2,4\*</sup>

<sup>1</sup>Graduate Institute of Systems Biology and Bioinformatics, National Central University, Chungli, Taiwan 32001. <sup>2</sup>Cathay Medical Research Institute, Cathay, General Hospital, Taipei, Taiwan. <sup>3</sup>Department of Chemical Engineering and Material, National Central University, Chungli, Taiwan 32001. <sup>4</sup>National Center for Theoretical Science, Shinchu, Taiwan 30043

### **Abstract**

A major challenge for post-genomics research is the integration of gene expressions with their corresponding regulatory elements and chromatin architectures on a genome-wide scale. Regulatory elements exert diverse mechanisms to regulate the expression of genes through protein-protein or protein-DNA interactions, while chromatin structures act in the upstream of the regulatory cascade and have a broad effect on the expression of multiple genes. Here, we employ a novel method, a genome-wide unrestrained functional elements assay (UFEA), to identify changes in regulatory elements and to pursue a comprehensive characterization of pathway enrichment of HCT-116 colorectal cancer cell line under Oxaliplatin treatment. Our experiments integrate high-resolution promoter tiling arrays, on samples that were treated with optimized concentration of DNase I, with exon arrays. Using methods including Starr and Siggene, two packages in "R", we identify from promoter array data 1709 genes with enriched promoter regions, from exon array 1037 genes differentially significantly expressed, and from combined data 564 genes enriched and significantly expressed, for pathway analysis. Our results show that: Oxaliplatin preferentially increases the binding intensities at promoter regions; the over-represented pathways are as likely to be up as are down regulated; those related to cancer form the largest group of down-regulated pathways; and the pathways of three neurodegenerative diseases, Huntington's, Parkingson's and Alzheimers's, all up-regulated, have by far the most statistically significant over-representation. These results suggest that UFEA is a useful method for genome-wide investigations of cis-acting regulatory elements.

**Author's Summary.** A novel method, a genome-wide unrestrained functional elements assay (UFEA), is employed to identify changes in regulatory elements and to pursue a comprehensive characterization of pathway enrichment of HCT-116 colorectal cancer cell line under Oxaliplatin treatment. Data from high-resolution promoter tiling arrays and exon arrays are analyzed in an integrated fashion and then enriched with information from KEGG and GO for insight in pathway activity. The general trend of our analysis is that many cancer related pathways are down-regulated whereas three neurodegenerative diseases, Huntington's, Parkingson's and Alzheimers's, are conspicuous among the upregulated pathways.

<sup>\*</sup> YAK and FHC are co-first authors; QL and HCL are co-corresponding authors.

### Introduction

Since the first hypersensitive site was identified over 31 years ago [1], approximately 100,000 DNase HS sites have been described in the literature. Evidence revealed that many DNase hypersensitive sites associate with regulatory regions including promoters, enhancers, silencers, insulators, and locus control regions, all related to gene expression [2]. DNase I is the enzyme of choice because of its high selectivity for nucleosome-free regions and relatively low DNA sequence specificity [3]. The change in chromatin structures is normally associated with transcriptional competence and can be detected as increased sensitivity to DNase I digestion. This increased sensitivity is referred to as DNase I-hypersensitivity [4]. The relationship between DNase I sensitivity and chromatin structure can be mutual and may even be effected by both epigenetic status and transcription activity [5, 6]. DNase I hypersensitive sites are often located in the recognition sites for transcription factors (TFs), including promoters and enhancers [4].

The traditional method for identifying DNase hypersensitive sites is Southern Blot [7]. In this method, an increasing amount of DNase I (or other restriction enzymes) is adopted to digest intact nuclei, and then blot probes for the regions of interest that might be hypersensitive sites.

Methods for identifying gene regulatory elements on a genome-wide scale include the ChIP-chip [8], DNase-chip [9-12] and ChIP-Seq [13]. Here we present a new method for monitoring changes in the whole-genome TF binding site and we correlate the results with gene expression profile. Our method, which we call unrestrained functional elements assay (UFEA), complements RNA transcription studies because, building on ChIP-chip and DNase-chip strategies to identify regulatory sites in intact chromatin, it enables the discovery of the presence of DNA-protein interactions that regulate gene expression. At low concentrations DNase I preferentially digests nucleosome-depleted DNA [14], whereas at high concentrations it is a unrestrained nuclease that cleaves DNA that is not bound by proteins. By correlating TF binding sites with the expression of their corresponding genes, this method can be used in conjunction with whole-genome tiling microarrays to investigate how DNA is regulated.

The main concept of non-restrained functional elements is as follows: Sequences unbound by proteins are digested thoroughly by application of DNase I at high concentrations. Proteins bound to the undigested sequences are then degraded by protease K causing previously bound DNA sequences to be released. The released DNA sequences, assumed to present loci of potential TF binding regions, are amplified and conjugated with promoter array. The results are analyzed, using algorithm including Starr [15], an open accessed package in "R", and combined with the gene expression microarray data (acquired using the same sample) and mapped to KEGG (Kyoto Encyclopedia of Genes and Genomes) [16, 17] and GO (Gene Ontology) [18] for insight in Oxaliplatin induced changes in functional regulatory pathways.

### **Materials and Methods**

**Cell line**. HCT-116, an epithelial-like cell line that comes from human colon carcinoma, was obtained from the American Type Culture Collection as a gift from Dr. C.J. Huang. The p26 HCT-116 cells were grown in DMEM (Gibco; pH 7.4) supplemented with 10% FBS (Gibco), 100 units/mL Penicillin/Streptomycin (Gibco) cultures. Cells were maintained at 37°C in a humidified atmosphere with 5% CO2. Cells were scraped down with 10 volumes

of Cell Lysis buffer (with protease inhibitors and DTT) to 1 volume of packed cells, which were around 107 cells in one plate. Cell numbers were determined using a Coulter counter (Coulter Electronic).

**Drug treatment**. Oxaliplatin stock solutions were made in water and stored at -20°C. Pilot studies had shown that the Pt-DNA levels were proportional to the drug concentration used over the range of 50 to 250  $\mu$ M. For each experiment, cells (107/10 ml medium in replicate 100-mm dishes) were exposed to 100  $\mu$ M Oxaliplatin. Growth activity was inhibited with this drug concentration followed by thirty minutes and one-hour incubations for the promoter and exon array assay experiments, respectively.

**DNase I unrestrained assay**. Nuclei were treated and tested under seven different concentrations of DNase I (Promega), from 5, 10, 20, 40, 60, 80, to 100 U/mL. Nuclei were treated 30 minutes at 37°C in 1mL volumes of DNase I buffer (60mM CaCl2, 750mM NaCl), the treatment ends with an equal volume of stop buffer (1M Tris-Cl, pH 8.0, 5M NaCl, 20% SDS, 0.5M EDTA, pH 8.0, 10 $\mu$ g/mL RNAseA) incubated at 65°C. Protease K was added to a final concentration of 25 $\mu$ g/mL into the DNase I treated nuclei and incubated overnight at 55°C. DNA is then purified with Puregene system (Gentra Systems, Minneapolis, MN) according to the manufacturer s protocol and resuspended in 10mM Tris-Cl, pH 8.0.

Arrays exercised in experiments. The Human Promoter 1.0R Array is composed of 4.6 million probes, tiled through over 25,500 human promoter regions. The average tiling resolution is 35 bps, 25-mer probes separated by 10-bp gaps. This array offers an extensive 10 kb coverage of approximately 7.5 kb upstream through 2.45 kb downstream relative to the 5' transcription start sites TSSs of approximately 25,000 human genes. Sequences were selected from NCBI human genome assembly (Build 34). Promoter regions were selected using sequence information from 35,685 Ensembl genes (version 21\_34d May 14, 2004), 25,172 RefSeq mRNAs (NCBI GenBank® February 7, 2004), and 47,062 complete-CDS mRNA (NCBI GenBank® December 15, 2003).

Human Exon 1.0 ST Array is composed of 5,362,207 features, which interrogate one million exon clusters with over 1.4 million probe sets from UCSC human assemblies (hg16, build 34). The Affymetrix GeneChip® Whole Transcript (WT) Sense Target Labeling Assay (Affymetrix Inc., Santa Clara, CA), is designed to generate amplified and biotinylated sense-strand DNA targets from the entire expressed genome without bias.

Microarray data acquisition and processing. Arrays were scanned using GeneChip® Scanner 3000 7G. We extracted signal intensities from the scanned images using a package in R named "Starr" for promoter array, and a software named "Expression Console Software (v.1.0) provided by Affymetrix for exon array. Further we use "siggene", a package in R version 2.10.1 program [15, 19, 20]. We used the mean intensity of each gene and regions that corresponded to each gene upon extraction, and converted signals into a scaled log ratio using the function: R(i) = Log (Experimental(i) / Control(i)).

**Microarray data process and integration**. Data analysis was carried out using the R statistical environment and programming language. We extensively used R software packages from Bioconductor [21], an open source bioinformatics resource. We used the 'Starr' and 'Siggene' packages written to handle Affymetrix data, and specifically the 'RMA' algorithm for pre-processing, normalization and calculation of expression values [22, 23].

## **Experimental Procedure**

The workflow of an UFEA-chip is summarized in Figure 2. Intact nuclei of HCT-116 are extracted and digested with DNase I, leaving behind only DNA covered by binding proteins. Proteins bound to DNA are then degraded by Protease K, and the remaining DNA fragments, which the experiment targets, are purified. The molecular mechanisms triggering an immediate response in the cell after treatment of, the action of Oxaliplatin have been previously described in several studies [24-30]. Here, HCT-116 colorectal cancer cells were treated with 100 µM Oxaliplatin, 30 minutes and 1 hour for promoter tiling array and exon array experiments, respectively. Both kinds of experiments were duplicated. The extracted nuclei were digested with 60 U/ml of DNase I (see below). The target DNA segments were amplified with PCR (following Affymetrix's protocol) and the resulting samples were applied to tiling arrays. Typically, a gene transcribed by RNA Polymerase II has a promoter region that extends for around 200 bp upstream from the TSS where TFs would bind [31]. The TF binding sites mostly lie within a range of 50 to 250 bp [32]. Thus the concentration of the DNase I (60 U/ml) used in this study was chosen so that the expected fragment size after PCR amplification lies between 100 and 300 bp. To each fragment 28 bp of Primer A are added at both ends.

### Results

Three promoter arrays, for the control and two treated samples, were processed with the methodology described above. Our hypothesis is that through this methodology, the analyzed results will yield, for every promoter-gene pair, information on protein binding regions in relation to the regulated gene. Enriched protein binding regions were detected through *Starr*, a Bioconductor package in R. In order to minimize cross-sample systematic errors we assume that the distribution of gene abundances is nearly the same in all samples and normalize the raw data through quantile normalization [33]. The normalized data were smoothed into bins of 250 bp. Using the quantile of the null distribution as an upper bound, a total 1709 enriched regions over the entire human genome were identified [19, 20, 22]. The regions are distributed over the chromosomes more or less in proportion

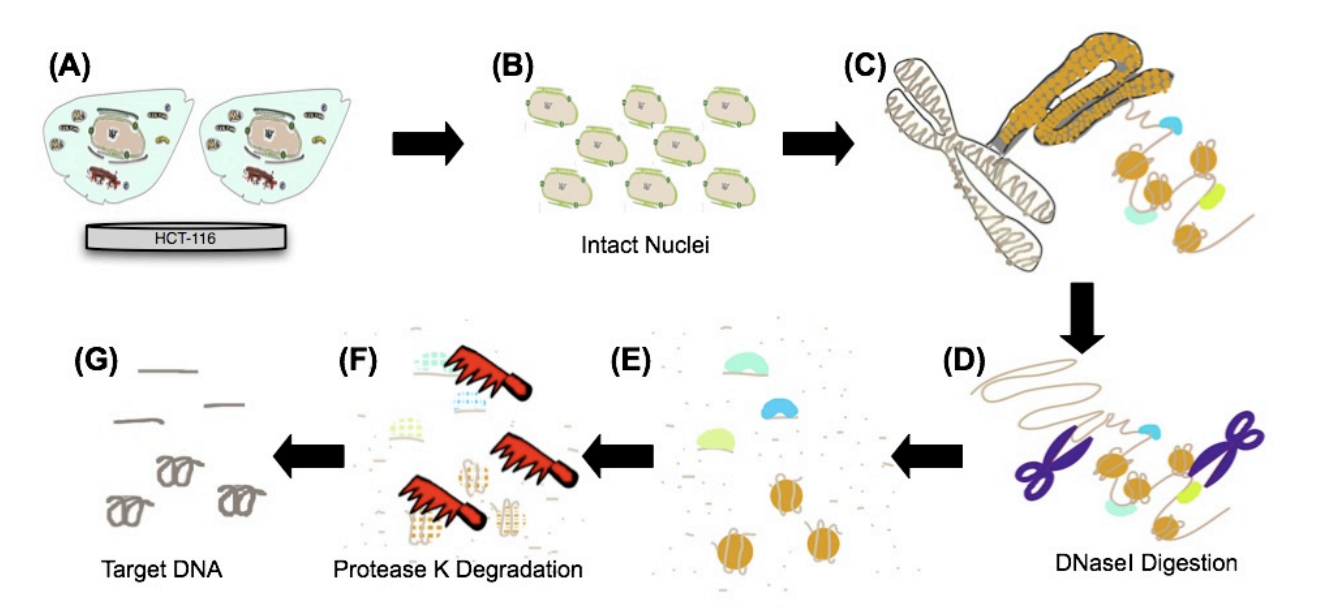


Figure 1. UFEA-chip Flowchart: Intact nuclei of HCT-116 are extracted (A-C) and digested with DNase I (D), proteins bound to DNA (E) are degraded by Protease K (F), and the remaining (target) DNA fragments (G) are purified.

to the gene density in the chromosomes and, to a lesser extent, to chromosome size (Figure 2). Figure 3 shows the intensity curves of enriched (promoter) regions in three representative types of relation between an enriched region and the ORF of the gene or

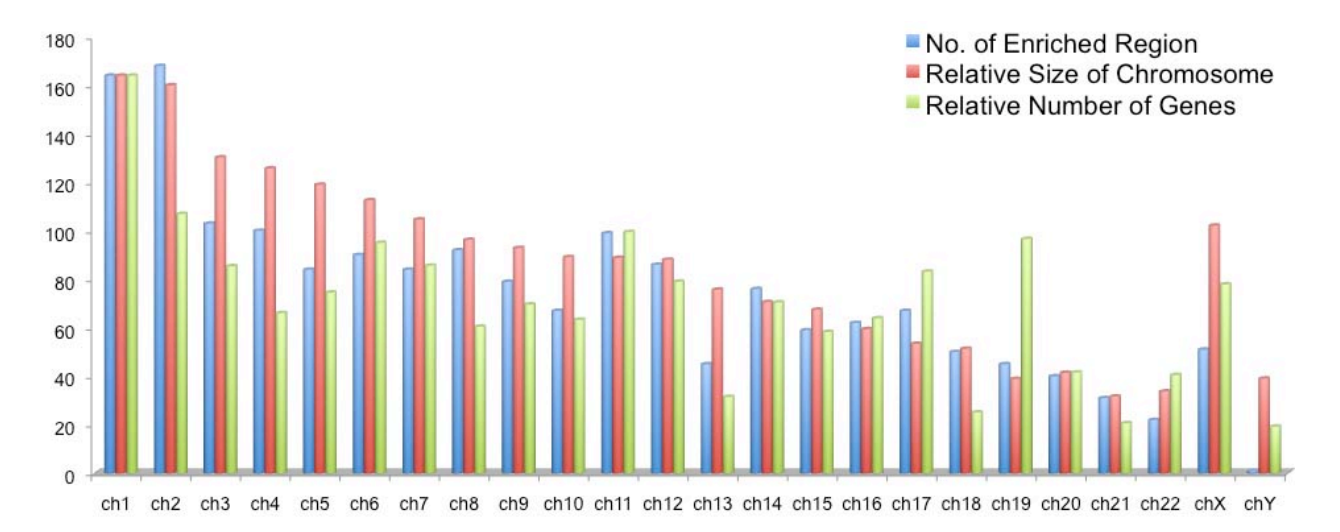
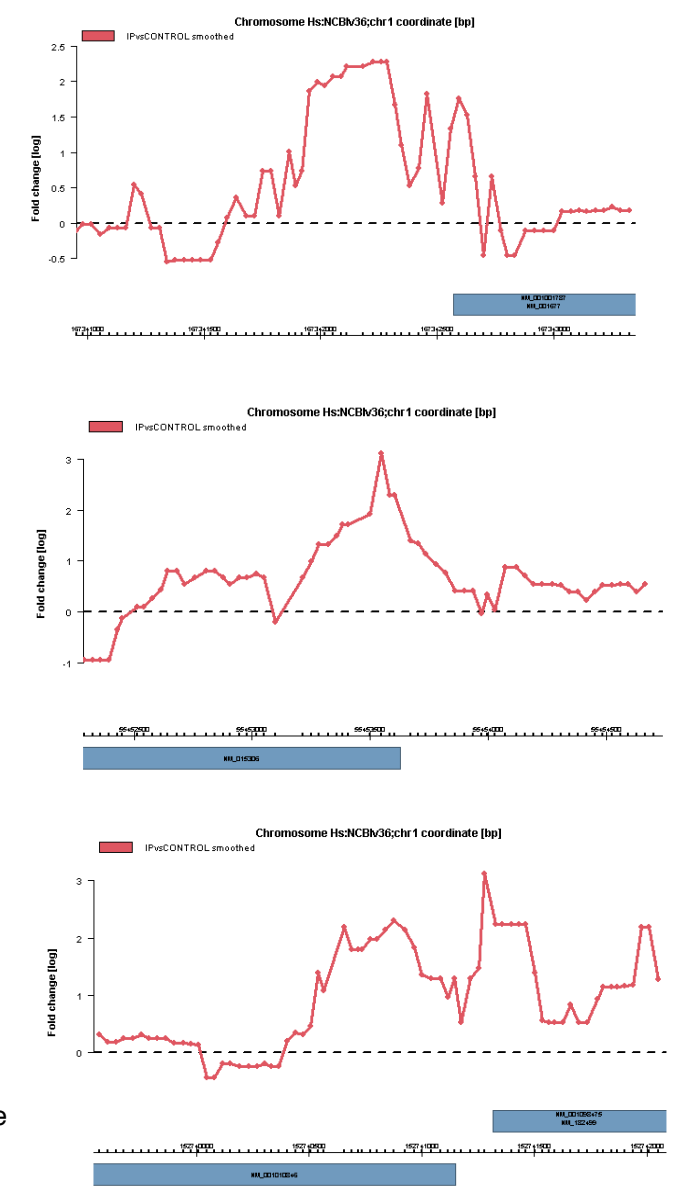


Figure 2. Distribution of 1709 enriched regions over individual chromosomes (blue) compared to relative sizes (red) of, and relative gene densities (green) in, chromosomes.

genes associated with that region: the gene is encoded on the positive strand, on the negative strand, and a pair of genes, one encoded in each strand. We call each of the plots shown in Figure 3 a protein binding profile (PBP). A common pattern of a PBP is that high intensity occurs in regions upstream of the gene (or genes in the third type) and near the 5'-end of the gene (or genes), whereas low intensity occurs near the 3'-end of the gene (or genes).

A statistical analysis of the intensity distribution of over a restricted promoter region (RPR) is shown in Figure 4. Here, an RPR, defined as beginning at 500 bp upstream from the TSS (of the gene associated with the promoter) and ending at 500 bp downstream from the transcription terminal site (TTS), is demarcated into ten overlapping blocks. Figure 4 shows the color coded mean intensity of each such block averaged over the 1709 enriched regions, 1681

Figure 3. Intensities (red) of enriched protein binding sites and ORFs (blue strips) of genes the corresponding promoters are supposed to regulate. (a) Regulated gene encoded on the positive strand; (b) regulated gene encoded on the negative strand; (c) genes encoded on both positive and negative strands.



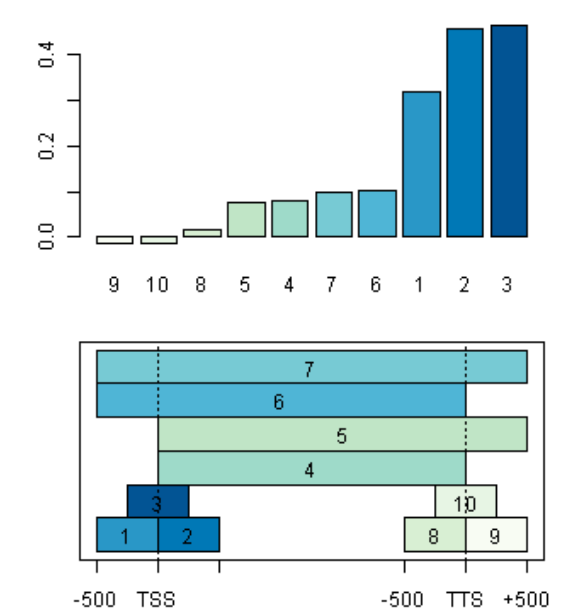


Figure 4. Lower panel: color coded mean intensities of blocks in averaged over the 1709 enriched regions. Upper panel: relative intensities of the ten blocks.

including 611 up-regulated uSEGs and 426 down-regulated dSEGs (Table S2, SI; see Figure S1 for a hierarchical clustering of the SEGs). The intersect of the set of 1709 PEGs and the set of 1037 SEGs contains 104 (51 up-regulated and 53 down-regulated) genes, all of whose promoter regions are over-enriched (Table S3, SI).

The intensities of promoters in block three (Figure 4a) from the promoter array and the intensities from the exon array of 16208 genes are plotted in Figure 5. The data display a slight skew towards up-regulation of the genes (mean intensity 0.03) and a strong skew towards over-enrichment (0.49). There are 8484 genes within a radius of 0.5 from the center of mass. We designate the four wedge-shaped sections exterior to the red circle and marked I, II, III, and IV, Figure 5, each spanning 30 degrees, as genes that are potentially both enriched and significantly expressed

over-enriched and 28 under-enriched (Table S1, Supporting Information (SI)). We call the genes corresponding to these enriched regions promoter enriched genes (PEGs) The mean intensity varies greatly. The intensities of blocks 1, 2 and 3, which lie within 500 bp of the TSS, are more than one order of magnitude greater than those of blocks 8, 9 and 10, which lie within 500 bp of the TTS.

Treated samples and controlled samples similar to those applied to promoter arrays were also applied to exon arrays. Data were analyzed through Siggene with the upper and lower cutoffs of 1.6 [20], and 1037 genes were identified as significant (differentially) expressed genes (SEG),

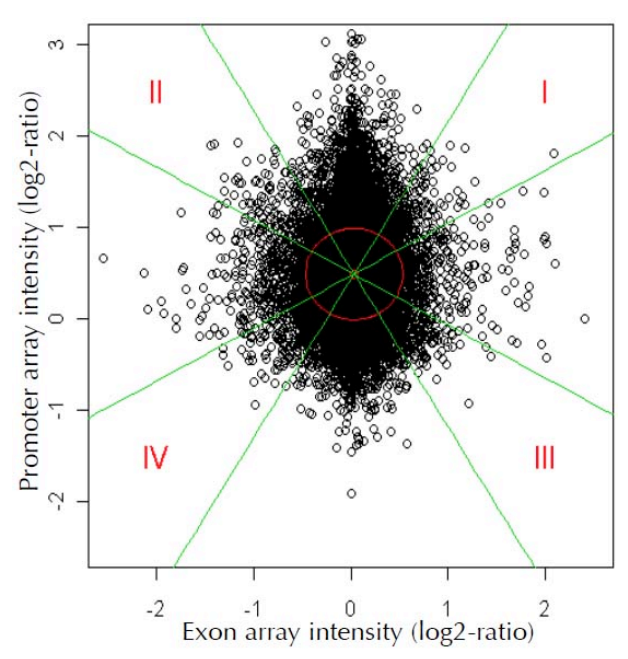


Figure 5. Promoter and exon array intensities of 16208 genes. The radius and center of the circle defining the excluded region, which contains 8484 genes, are 0.5 and (0.03, 0.49), respectively. Each of the wedges delineating the four sections I, II, III and IV span 30 degrees. The number of genes in the sections are: I, 297; II, 267; III, 358; IV, 336.

events: I, over-enriched (oP) and up-regulated (uX) and contains 297 genes; II, oP and down-regulated (dX), 267 genes; III, under-enriched (nP) and uX, 358 genes; IV, nP and dX, 336 genes (Table S4, SI). However, owing to the over-enrichment of the promoter data, most of the genes in segments III and IV are not or at most only slightly under-enriched. We therefore view genes in these segments as rare but not significant events and do not subject them to further analysis.

The four sets of genes, 611 uSEGs, 426 dSEGs, 297 oP-uXs, and 267 oP-dXs, were mapped to KEGG (Kyoto Encyclopedia of Genes and Genomes) [16, 17] and GO (Gene Ontology) [18] for over-representation according to biological function. The number of over-represented (with P value less than 0.05) pathways for the four gene sets are uSEG, 17; dSEG, 17; oP-uR, 5; and oP-dX, 5. Results are shown in Tables 1, where for pathways ranked below 13 are not shown. Over-represented pathways deduced from PEGs are given in Table S5, SI.

Table 1: KEGG pathways in which PEGs and SEGs are over-represented. uPEG and dPEG, over- and under enriched PEG, respectively; uSEG and dSEG, up- and down-regulated SEG, respectively. All pathways have P values (for over-representation) less than 0.05. Only the top 13 of uSEG and dSEG (both have 17) pathways are listed.

uSEG	KEGGID	P value	Odds Ratio	Exp Count	Count	Size	"Term"
1	190	1.03E-13	8.65	4.15	25	106	Oxidative phosphorylation
2	5012	3.76E-12	7.95	4.03	23	103	Parkinson's disease
3	5016	2.39E-10	5.45	6.23	26	159	Huntington's disease
4	5010	3.55E-08	4.79	5.76	22	147	Alzheimer's disease
<del></del> 5	3050	2.01E-06	8.61	1.57	10	40	Proteasome
6	3040	7.81E-06	4.26	4.50	16	115	Spliceosome
7	1100	1.70E-04	1.85	39.19	60	1001	Metabolic pathways
8	4115	1.70E-04 1.06E-03	3.96	2.62		67	
					9		p53 signaling pathway
9	3020	3.48E-03	5.71	1.06	5	27	RNA polymerase
10	240	8.71E-03	2.78	3.56	9	91	Pyrimidine metabolism
11	4110	2.04E-02	2.26	4.78	10	122	Cell cycle
oP-uX					_		
1	190	2.82E-04	5.41	1.73	8	106	Oxidative phosphorylation
2	5012	1.29E-03	4.67	1.68	7	103	Parkinson's disease
3	5016	3.98E-03	3.47	2.59	8	159	Huntington's disease
4	5010	9.42E-03	3.23	2.39	7	147	Alzheimer's disease
5	3040	3.84E-02	2.87	1.87	5	115	Spliceosome
dSEG							
1	4520	1.31E-06	6.84	2.20	12	74	Adherens junction
2	4510	1.12E-05	3.75	5.70	18	192	Focal adhesion
3	5200	4.46E-05	2.88	9.41	23	317	Pathways in cancer
4	4120	2.88E-04	3.71	3.71	12	125	Ubiquitin mediated proteolysis
5	4310	1.11E-03	3.14	4.31	12	145	Wnt signaling pathway
6	5412	1.30E-03	4.21	2.17	8	73	Arrhythmogenic right ventricular
7	4330	1.51E-03	5.50	1.28	6	43	Notch signaling pathway
8	4350	2.75E-03	3.69	2.44	8	82	TGF-beta signaling pathway
9	5222	2.75E-03	3.69	2.44	8	82	Small cell lung cancer
10	5215	4.28E-03	3.41	2.61	8	88	Prostate cancer
11	5212	4.76E-03	3.71	2.11	7	71	Pancreatic cancer
12	5223	4.91E-03	4.23	1.60	6	54	Non-small cell lung cancer
13	4810	7.05E-03	2.35	6.06	13	204	Regulation of actin cytoskeleton
oP-dX							
1	4150	5.44E-03	6.29	0.72	4	51	mTOR signaling pathway
2	4114	1.67E-02	3.64	1.51	5	107	Oocyte meiosis
3	4810	2.35E2	2.67	2.87	7	204	Regulation of actin cytoskeleton

4	4120	3.04E-02	3.08	1.76	5	125	Ubiquitin mediated proteolysis
5	5213	3.61E-02	4.45	0.73	3	52	Endometrial cancer

The mechanism of platinum drug toward cancer is mediated through the combined processes of cell entry, drug activation, DNA-binding, and transcription inhibition. Oxaliplatin binds nuclear DNA to form Pt-DNA cross-links that arrest key cellular functions and activate responses such as DNA repair [34].

All cancer related pathways, one of 11 of 13 in the dSEG set and 2 in 5 in set oP-dX, are associated with down-regulation of genes. In the dSEG set, 3 and 9-12 are cancer pathways; 1 and 2, related cell adhesion, are pathways for metastasis; 5, 7, and 8, the signaling pathways, are related to proliferation and cell division. Pathway 4 is not specifically cancer and 13 is not related to cancer.

There are a total five neurodegenerative disease pathways in KEGG database. Three, Huntington's, Parkinson's, and Alzheimer's (HPA), are activated and the other two are not. Also activated is the metabolic oxidative phosphorylation pathway (OP), which in fact is a sub-pathway of each of the HPA pathways, but not of the other two (amyotrophic lateral sclerosis and prion diseases). In HPA and OP, the common activated genes are those forming the five gene complexes, complexes I through V, in mitochondria.

Pyrimidine metabolism, another of the activated pathways, is related to neurodegeneration when thiamine deficiency occurs [35].

The proteasome and spliceosome pathways are involved in the manufacturing of DNA elements and the supply of components for transcriptions. These are not closely related to metabolism as they require very little ATP. Their activation may be in response to the damage to DNA caused by the application of Oxaliplatin.

### Discussion

About 98% of the differentially enriched promoter regions are over-enriched, thus indicating Oxaliplatin as an overwhelming activator. A large majority of the pathways over-represented by differentially down-regulated genes are cancer related, this confirms Oxaliplatin as a cancer suppressing drug, its designated purpose. Pathways in the oP-dX set in Table 1, including the mTOR signaling and endometrial cancer pathways, are associated with down-regulated genes but over-enriched promoter regions. This suggests that the associated promoter regions may be binding sites of suppressor factors, or TFs that suppress the activities of pathways [36]. The pathways most over-represented by far by up-regulated genes are related to neurodegenerative diseases and oxidative phosphorylation, all connected to the activation of some or all of the respiratory complexes I to V within the inner membrane of mitochondria. Oxaliplatin is known to cause neuropathy [37, 38] and, separately, severe mitochondrial dysfunction (through Bax and Bak activation) [27]. In one experiment on rat it was validated that the severity of neuropathy induced by Oxaliplatin was lowered when the mitochondrial complexes I and III are blocked [39].

Our study suggests a more detailed sequence of events as follows. The cytotoxicity of platinum compounds in Oxaliplatin causes inhibition of DNA synthesis in cancer cells, as is manifest in the down-regulation of many genes involved in cancer-related signaling pathways, including Wnt signaling pathway, Notch signaling pathway and TGF-beta

signaling pathway (Table 1). At the same time, genes not directly related cancer, such as those encoding the three proteins, the solute carrier family 6 (neurotransmitter transporter, taurine), member 6 (SLC6A6), huntington disease protein (HTT), and Amyloid beta protein precursor (APP), are also down-regulated (Table S2, SI; all with P value less than 0.02). Previous studies showed that these three proteins, SLC6A6, HTT, and APP may have important functions in tumor progression [27, 40-42]. When activated these proteins lead to inhibition of the respiratory complexes (I, II, and IV, respectively) within the inner membrane of mitochondria, which (when active) play critical roles in initiating the neurodegenerative Parkinson's, Huntington's, and Alzheimer's diseases (Figures S2-4; SI), respectively. The suppression of the three proteins induced by Oxaliplatin leads to overactivation of the respiratory complexes, increased levels of ROS, and then Ca<sup>2+</sup>, then the falling of membrane potentials in mitochondria, and ultimately cell death. Oxaliplatin induced mitochondrial apoptotic response to colon carcinoma cells has been reported [27].

An intriguing aspect in our study is the lack of strong correlation between the PEG and SEG sets of genes: genes corresponding to the most over- or under-enriched promoter regions tend not to be the most significantly up- or down-regulated genes. One possible cause is the lack of synchronicity of promoter activity and gene expression. Another could be that because in the Human Promoter 1.0R Array use here the promoter region starts at about 7.5 kb upstream of the TSS of a gene, some enriched promoter regions signify regulation of expression not of genes, but of noncoding DNA [43]. This possibility needs to be further explored. Our study shows that UFEA is a simple and practical method for gaining information on differential binding activity in promoter regions over the entire genome under drug administration that can be used to gain insight on the activation of biological pathways.

# **Funding**

This work was partly funded by the National Science Council (ROC) (http://web1.nsc.gov.tw/mp.aspx?mp=7), the Cathy General Hospital (http://www.cgh.org.tw/en/index.html), and the National Central University (http://www.ncu.edu.tw/e\_web/index.php). The funders had no role in study design, data collection and analysis, decision to publish, or preparation of the manuscript.

# **Supporting Information**

http://sansan.phy.ncu.edu.tw/~hclee/mtg/recomb2010/SupportingInformation.pdf

# **Bibliography**

- 1. Jongstra, J., et al., *Induction of altered chromatin structures by simian virus 40 enhancer and promoter elements.* Nature, 1984. **307**(5953): p. 708-14.
- 2. Hutchison, N. and H. Weintraub, *Localization of DNAase I-sensitive sequences to specific regions of interphase nuclei.* Cell, 1985. **43**(2 Pt 1): p. 471-82.
- 3. Dingwall, C., G.P. Lomonossoff, and R.A. Laskey, *High sequence specificity of micrococcal nuclease*. Nucleic Acids Res, 1981. **9**(12): p. 2659-73.
- 4. Gross, D.S. and W.T. Garrard, *Nuclease hypersensitive sites in chromatin*. Annu Rev Biochem, 1988. **57**: p. 159-97.

- 5. Kang, S.H., C.M. Kiefer, and T.P. Yang, *Role of the promoter in maintaining transcriptionally active chromatin structure and DNA methylation patterns in vivo.* Mol Cell Biol, 2003. **23**(12): p. 4150-61.
- 6. Gilbert, N. and B. Ramsahoye, *The relationship between chromatin structure and transcriptional activity in mammalian genomes.* Brief Funct Genomic Proteomic, 2005. **4**(2): p. 129-42.
- 7. Cartwright, I.L. and S.C. Elgin, *Nucleosomal instability and induction of new upstream protein-DNA associations accompany activation of four small heat shock protein genes in Drosophila melanogaster.* Mol Cell Biol, 1986. **6**(3): p. 779-91.
- 8. Ren, B., et al., *Genome-wide location and function of DNA binding proteins*. Science, 2000. **290**(5500): p. 2306-9.
- 9. Sabo, P.J., et al., *Genome-wide identification of DNasel hypersensitive sites using active chromatin sequence libraries.* Proc Natl Acad Sci U S A, 2004. **101**(13): p. 4537-42.
- 10. Sabo, P.J., et al., *Genome-scale mapping of DNase I sensitivity in vivo using tiling DNA microarrays.* Nat Methods, 2006. **3**(7): p. 511-8.
- 11. Dorschner, M.O., et al., *High-throughput localization of functional elements by quantitative chromatin profiling.* Nat Methods, 2004. **1**(3): p. 219-25.
- 12. Attanasio, C., et al., *Assaying the regulatory potential of mammalian conserved non-coding sequences in human cells.* Genome Biol, 2008. **9**(12): p. R168.
- 13. Johnson, D.S., et al., *Genome-wide mapping of in vivo protein-DNA interactions*. Science, 2007. **316**(5830): p. 1497-502.
- 14. Segal, E., et al., *A genomic code for nucleosome positioning.* Nature, 2006. **442**(7104): p. 772-8.
- 15. Toedling, J., et al., *Ringo--an R/Bioconductor package for analyzing ChIP-chip readouts*. BMC Bioinformatics, 2007. **8**: p. 221.
- 16. Kanehisa, M., *A database for post-genome analysis.* Trends Genet, 1997. **13**(9): p. 375-6.
- 17. Heiman, M., et al., *A translational profiling approach for the molecular characterization of CNS cell types.* Cell, 2008. **135**(4): p. 738-48.
- 18. Ashburner, M., et al., *Gene ontology: tool for the unification of biology. The Gene Ontology Consortium.* Nat Genet, 2000. **25**(1): p. 25-9.
- 19. Zacher, B., P.F. Kuan, and A. Tresch, *Starr: Simple Tiling ARRay analysis of Affymetrix ChIP-chip data.* BMC Bioinformatics. **11**: p. 194.
- 20. Holger Schwender, A.K., and Katja Ickstadt, *Comparison of the Empirical Bayes* and the Significance Analysis of Microarrays.
- 21. Gentleman, R.C., et al., *Bioconductor: open software development for computational biology and bioinformatics.* Genome Biol, 2004. **5**(10): p. R80.
- 22. Irizarry, R.A., et al., *Exploration, normalization, and summaries of high density oligonucleotide array probe level data.* Biostatistics, 2003. **4**(2): p. 249-64.
- 23. Irizarry, R.A., et al., *Summaries of Affymetrix GeneChip probe level data.* Nucleic Acids Res, 2003. **31**(4): p. e15.
- 24. Arango, D., et al., *Molecular mechanisms of action and prediction of response to oxaliplatin in colorectal cancer cells.* Br J Cancer, 2004. **91**(11): p. 1931-46.
- 25. Raymond, E., et al., *Cellular and molecular pharmacology of oxaliplatin.* Mol Cancer Ther, 2002. **1**(3): p. 227-35.
- 26. Plasencia, C., et al., *Expression analysis of genes involved in oxaliplatin response and development of oxaliplatin-resistant HT29 colon cancer cells.* Int J Oncol, 2006. **29**(1): p. 225-35.
- 27. Gourdier, I., et al., *Oxaliplatin-induced mitochondrial apoptotic response of colon carcinoma cells does not require nuclear DNA*. Oncogene, 2004. **23**(45): p. 7449-57.

- 28. Woynarowski, J.M., et al., *Oxaliplatin-induced damage of cellular DNA.* Mol Pharmacol, 2000. **58**(5): p. 920-7.
- 29. Boyer, J., et al., *Pharmacogenomic identification of novel determinants of response to chemotherapy in colon cancer.* Cancer Res, 2006. **66**(5): p. 2765-77.
- 30. Voland, C., et al., Repression of cell cycle-related proteins by oxaliplatin but not cisplatin in human colon cancer cells. Mol Cancer Ther, 2006. **5**(9): p. 2149-57.
- 31. Lewin, B., Genes VIII 2004: p. 1056.
- 32. Moss, T., *DNA-protein interactions: principles and protocols.* 2 ed. 2001: Humana Press. 638.
- 33. Bolstad, B.M., et al., *A comparison of normalization methods for high density oligonucleotide array data based on variance and bias.* Bioinformatics, 2003. **19**(2): p. 185-93.
- 34. Ahmad, S., *Platinum-DNA interactions and subsequent cellular processes controlling sensitivity to anticancer platinum complexes.* Chem Biodivers. **7**(3): p. 543-66.
- 35. Boss, G.R. and J.E. Seegmiller, *Genetic defects in human purine and pyrimidine metabolism.* Annu Rev Genet, 1982. **16**: p. 297-328.
- 36. Rowland, B.D. and D.S. Peeper, *KLF4, p21 and context-dependent opposing forces in cancer.* Nat Rev Cancer, 2006. **6**(1): p. 11-23.
- 37. Wang, D. and S.J. Lippard, *Cellular processing of platinum anticancer drugs.* Nat Rev Drug Discov, 2005. **4**(4): p. 307-20.
- 38. Park, S.B., et al., *Oxaliplatin-induced neurotoxicity: changes in axonal excitability precede development of neuropathy.* Brain, 2009. **132**(Pt 10): p. 2712-23.
- 39. Joseph, E.K. and J.D. Levine, *Comparison of oxaliplatin- and cisplatin-induced painful peripheral neuropathy in the rat.* J Pain, 2009. **10**(5): p. 534-41.
- 40. Meng, J.Y., et al., *Amyloid beta protein precursor is involved in the growth of human colon carcinoma cell in vitro and in vivo*. Int J Cancer, 2001. **92**(1): p. 31-9.
- 41. Steffan, J.S., et al., *The Huntington's disease protein interacts with p53 and CREB-binding protein and represses transcription.* Proc Natl Acad Sci U S A, 2000. **97**(12): p. 6763-8.
- 42. Mochizuki, T., H. Satsu, and M. Shimizu, *Signaling pathways involved in tumor necrosis factor alpha-induced upregulation of the taurine transporter in Caco-2 cells.* FEBS Lett, 2005. **579**(14): p. 3069-74.
- 43. Elgar, G. and T. Vavouri, *Tuning in to the signals: noncoding sequence conservation in vertebrate genomes.* Trends Genet, 2008. **24**(7): p. 344-52.